Supplementary Information to: In-atmosphere production makes a negligible contribution to global emissions of HFC-23

Ben Adam[1], Rayne Holland[1], Daniel Van Hoomissen[2], James B. Burkholder[2], Anwar Khan[1], Paul Griffiths[1], Jens Mühle[3], Dudley Shallcross[1], and Matt Rigby[1]

[1]School of Chemistry, University of Bristol, Bristol, United Kingdom
[2]Chemical Sciences Laboratory, National Oceanic and Atmospheric Administration (NOAA), 325 Broadway, Boulder, CO 80305-3328, USA
[3]Scripps Institution of Oceanography, University of California San Diego, La Jolla, CA, USA

Correspondence: Ben Adam (benjamin.adam@bristol.ac.uk)

S1 Supplementary Tables

Table S1. List of all model runs in the sensitivity study and the parameters used. The columns show the quantum yield parametrization (photolysis), the dry deposition velocity (V_d), the convective and dynamic scavenging coefficients (SC), total HFO emissions (E_{HFO}) and their spatial distribution (spatial distribution), the CF_3CHO absorption cross section (AXS) and whether or not the reversible reaction between CF_3CHO and HO_2 was included (HO_2). The JPL cross-section can be found in Burkholder et al. (2019).

run	**photolysis**	**V_d / cm s^{-1}**	**SC / cm^{-1}**	**E_{HFO} / Gg yr^{-1}**	**spatial distribution**	AXS	HO_2
base	base	0.01	3.0	19.0	modified EDGAR	JPL	No
Phot_Hi	PhotHi	0.01	3.0	19.0	modified EDGAR	JPL	No
Phot_Low	PhotLow	0.01	3.0	19.0	modified EDGAR	JPL	No
Em_Low	base	0.01	3.0	6.3	modified EDGAR	JPL	No
Em_Hi	base	0.01	3.0	57.0	modified EDGAR	JPL	No
Scav_1	base	0.01	1.0	19.0	modified EDGAR	JPL	No
Scav_5	base	0.01	5.0	19.0	modified EDGAR	JPL	No
Scav_7	base	0.01	7.0	19.0	modified EDGAR	JPL	No
Scav_10	base	0.01	7.0	19.0	modified EDGAR	JPL	No
Dep_0.001	base	0.001	3.0	19.0	modified EDGAR	JPL	No
Dep_0.1	base	0.1	3.0	19.0	modified EDGAR	JPL	No
Dep_1	base	1.0	3.0	19.0	modified EDGAR	JPL	No
Dep_10	base	10.0	3.0	19.0	modified EDGAR	JPL	No
Dist_flatland	base	0.01	3.0	19.0	uniform over land only	JPL	No
Dist_flatlandsea	base	0.01	3.0	19.0	uniform over land and sea	JPL	No
Dist_polar	base	0.01	3.0	19.0	uniform at latitudes > 60°N/S	JPL	No
Dist_equator	base	0.01	3.0	19.0	uniform at latitudes < 30°N/S	JPL	No
AXS_Hi	base	0.01	3.0	19.0	modified EDGAR	JPL + 10%	No
AXS_Low	base	0.01	3.0	19.0	modified EDGAR	JPL - 10%	No
HO_2	base	0.01	3.0	19.0	modified EDGAR	JPL	Yes

Table S2. Direct and indirect global warming potentials for each of the eight source gases considered in the model, across the twenty-, one-hundred- and five-hundred-year time horizons (GWP_{20}, GWP_{100} and GWP_{500}). Values of the direct GWP_{100} are taken from Burkholder et al. (2022), while the mean and standard deviation of the indirect GWP_{100} values calculated across the twenty model runs are presented here.

species	**Direct GWP$_{20}$**	**Indirect GWP$_{20}$**	**Direct GWP$_{100}$**	**Indirect GWP$_{100}$**	**Direct GWP$_{500}$**	**Indirect GWP$_{500}$**
HFC-143a	7900	1.13 ± 0.08	5900	4.3 ± 0.3	1980	1.2 ± 0.1
HFC-236fa	7820	0.15 ± 0.01	9120	0.81 ± 0.06	6340	0.23 ± 0.02
HFC-245fa	3190	1.4 ± 0.1	966	2.3 ± 0.2	276	0.65 ± 0.05
HFC-365mfc	3100	1.65 ± 0.11	969	2.8 ± 0.2	276	0.79 ± 0.06
HFO-1234ze(E)	4	7.3 ± 0.3	1	8.5 ± 0.4	< 1	2.4 ± 0.1
HFO-1336mzz(Z)	9	6.1 ± 0.4	2	7.1 ± 0.5	< 1	2.0 ± 0.1
HCFO-1233zd(E)	14	6.2 ± 0.3	4	7.2 ± 0.3	1	2.1 ± 0.1

S2 Supplementary Figures

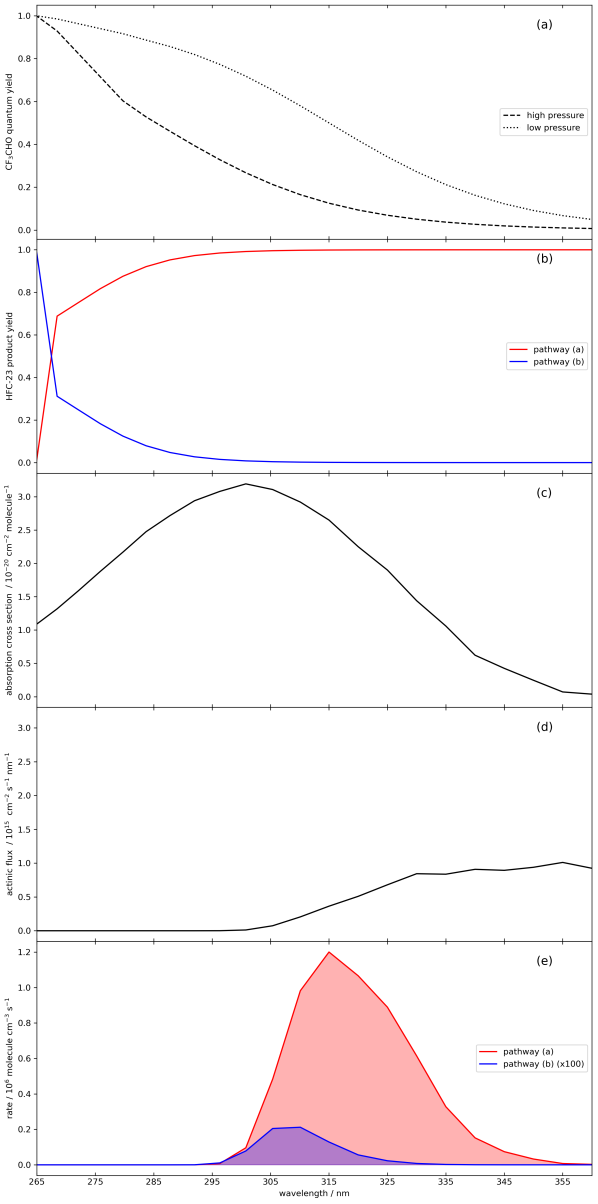

Figure S1. (a) Variation with wavelength of the CF_3CHO photolysis quantum yield in the model, according to equation 1 in the main text. The dashed line shows the quantum yield calculated at the highest pressure in the model, while the dotted line shows the quantum yield at the lowest pressure in the model. These are also the pressures used in the 'Phot_Hi' and 'Phot_Low' scenarios. The quantum yield is set to 0.5 for wavelengths below 266 nm and 0 for wavelengths longer than 360 nm. (b) Variation with wavelength of the photolysis product yield for HFC-23 with wavelength. Pathway (a), producing radicals, is shown in red and is calculated as one minus the HFC-23 product yield, while the HFC-23 product yield (pathway (b)) is shown in blue. While this quantity varies slightly with pressure, this is insignificant and not shown here. (c) Variation with wavelength of the absorption cross-section of CF_3CHO used in the model. (d) Typical surface actinic flux used in the model. (e) Contribution of each wavelength to the overall photolysis rate at the surface for pathways (a) and (b), shown in red and blue respectively. The contribution of pathway (b) is shown at 100x enlargement. This is calculated as the product of the quantum and product yields, the absorption cross-section and actinic flux. The area under each of the lines corresponds to the overall photolysis rate, as discussed in the main manuscript.

References

Burkholder, J., Abbatt, J., Cappa, C., Dibble, T., Kolb, C., Orkin, V., Wilmouth, D., Sander, S., Barker, J., Crounse, J., Huie, Kurylo, M., Percival, C., and Wine, P.: JPL Publication 19-5. Chemical Kinetics and Photochemical Data for Use in Atmospheric Studies, Tech. rep., Jet Propulsion Laboratory, Pasadena, CA, 2019.

Burkholder, J., Hodnebrog, Ø., McDonald, B., Orkin, V., Papadimitriou, V., and Van Hoomissen, T.: Annex : Summary of Abundances, lifetimes, ODPs, REs, GWPs, and GTPs, in: Scientific Assessment of Ozone Depletion 2022, no. 278 in Global Ozone Research and Monitoring Project, pp. 435–492, World Meteorological Organization, Geneva, Switzerland, https://ozone.unep.org/system/files/documents/Scientific-Assessment-of-Ozone-Depletion-2022.pdf, 2022.